Journal of Alloys and Compounds, 206 (1994) 237–242
JALCOM 1044

Kinetics and mechanism of the oxidation of ZrC

G.A. Rama Rao and V. Venugopal*
Fuel Chemistry Division, Bhabha Atomic Research Centre, Bombay 400094 (India)

(Received November 5, 1993)

Abstract

The oxidation behaviour of sintered ZrC powder was studied under iso- and non-isothermal heating conditions under varied oxygen pressures from 5 to 50 kPa and the weight changes during the reaction were followed by thermogravimetry. The sample ignited under an oxygen pressure of 101.3 kPa when heated non-isothermally at 5 K min^{-1}. The end product was identified by X-ray diffraction as cubic ZrO_2 at temperatures below 1073 K and monoclinic above that. The rate of the reaction was found to be diffusion controlled. The mechanism of the reaction was discussed in terms of the diffusion of oxygen through the product layer.

1. Introduction

Zirconium is one of the high yielding fission products during the fission of ^{235}U and ^{239}Pu. In a mixed carbide fuel it is found to be monophasic, soluble in UC [1]. The oxidation behaviour of ZrC and (U, Zr)C needs to be understood if oxidation is to be considered as a head-end step during reprocessing. The oxidation reaction of zirconium carbide to oxide was reported to proceed through zirconium oxycarbide as an intermediate phase [2–5]. Barnier and Thevenot [2] studied the oxidation under 13 kPa oxygen pressure in the temperature range 673–1273 K. Afomin *et al.* [3] carried out the oxidation on sintered ZrC under 3–2660 Pa of oxygen pressure in the range 973–1773 K. Shimada and Ishii [4] varied the oxygen pressure from 0.66 to 39.5 K Pa under static conditions in the temperature range 653–823 K. Bartlett *et al.* [5] suggested a rapid surface reaction under 101.3 kPa of oxygen pressure above 723 K. Zhilyaev and Askarova [6] studied the oxidation reaction under the oxygen pressures obtained from NiO but formation of oxycarbide was not reported. Shevchenko *et al.* [7] oxidized ZrC powder in the range 773–1073 K and proposed the mechanism as that of oxygen diffusion controlled with oxycarbide as the intermediate product. Kuriakose and Margrave [8] proposed a linear rate for the oxidation of ZrC powder in the range 827–925 K under 99.2 kPa oxygen pressure. The pressure variation in the published work under isothermal heating conditions ranged from 0.66 to 101.3 kPa with corresponding variation in mechanism from diffusion-controlled to linear reaction. The activation energies reported recently by Shimada and Ishii [4] did not match those reported earlier [2, 5] under similar oxygen pressures. The present work is aimed at the study of the mechanism of the non-isothermal oxidation reaction on sintered ZrC powder under varying oxygen pressure from 5 to 50 kPa and we propose a mechanistic model to explain the stabilization of cubic ZrO_2 phase at room temperature.

2. Theory

2.1. Mechanism

2.1.1. Oxidation

Shimada and Ishii [4] studied the oxidation under isothermal conditions and suggested that the conversion of ZrC to ZrO_2 proceeded according to the equation

$$ZrC(s)+2O_2(g) \longrightarrow ZrO_2(s)+CO_2(g) \qquad (1)$$

The atomic oxygen displaces carbon in the interstitial vacancies of the ZrC lattice, forming $Zr(C_xO_y)$. The initial weight increase is due to the formation of such an intermediate with oxygen up to $y=0.6$. The formation was very rapid in the initial stages and was controlled by a diffusion process. The rate-governing process was described by Jander's diffusion model with a rate-governing equation

$$kt=[1-(1-\alpha)^{1/3}]^2 \qquad (2)$$

where α is the reacted fraction, k the rate constant and t the reaction time.

In this study it was assumed that (1) nucleation, followed by surface diffusion, occurs at lower temper-

---

*Author to whom correspondence should be addressed.

SSDI 0925-8388(93)01044-5

atures resulting in the formation of a coherent product layer, (2) the surface of the substrate is covered and (3) bulk diffusion is unidirectional and the volume ratios of the product and the reactant do not change.

2.1.2. Isothermal and non-isothermal kinetics

Attempts were made to fit the data obtained during the isothermal heating conditions into various kinetic equations with the help of a computer program. Activation energies and pre-exponential factors were calculated from the log k *vs.* $1/T$ plots. The data on non-isothermal oxidation were evaluated by the method suggested by Zsako [9] using a computer program developed by Ravindran [10]. The basic equation for the integral methods of analysis of thermoanalytical curves proposed by Doyle [11] for non-isothermal studies is given by

$$g(\alpha) = ZEp(x)/qR \qquad (3)$$

where $g(\alpha)$ is a function of α, the fraction reacted, and $p(x)$ is a function of x defined as $x = E/RT$. Z, E, R, q and T are respectively the pre-exponential factor of the Arrhenius equation, the activation energy, the gas constant, the heating rate and the absolute temperature.

Zsako [9] and Skvara and Satava [12] used eqn. (3) in logarithmic form:

$$\ln g(\alpha) - \ln p(x) = \ln ZE/qR \qquad (4)$$

which implies that the plots of $\ln g(\alpha)$ *vs.* T and $\ln p(x)$ *vs.* T should be identical in shape, provided that the assumed mechanism for the calculation of $g(\alpha)$ and the activation energy for the calculation of $p(x)$ are correct. The probable mechanism is that for which the standard deviation is at a minimum for a particular combination of activation energy and a reaction mechanism.

3. Experimental details

Sintered ZrC powder (99%; surface area, 0.7 $m^2\,g^{-1}$, density, 6.73 $g\,cm^{-3}$) was obtained from Aldrich Chemical Company. The thermogravimetric runs were recorded on a Sinku Rico thermal analyser with an IR gold image furnace at 10 μg sensitivity. The sample mass for each experiment was around 25 mg. The partial pressure of oxygen was maintained at 5, 20 and 50 kPa by mixing with argon under flowing conditions. The heating rate for non-isothermal conditions was varied from 5 to 15 K min^{-1} in the temperature range 550–1300 K. In the case of isothermal experiments, the sample was heated in argon atmosphere to the desired temperature and the reacting gas was introduced. The isothermal experiments were carried out at 20 kPa oxygen pressure in the temperature range 750–810 K.

4. Results and discussion

The possible reactions that occur during the conversion of ZrC to ZrO_2 are given as

$$ZrC(s) + \tfrac{3}{2}(1-x)O_2(g) \longrightarrow ZrC_xO_{1-x} + (1-x)CO_2 \qquad (5)$$

$$ZrC_xO_{1-x} + [(1+3x)/2]O_2(g) \longrightarrow ZrO_2 + xCO_2(g) \qquad (6)$$

The product at various stages of the reaction was analysed for carbon and was found to have been associated with free carbon. The colour of the product was also black. The plot of sample mass variation with temperature for the non-isothermal heating of the sample with respect to the variation in oxygen pressure is given in Fig. 1. The total mass gain observed at the end of the experiment was larger than would be expected if the reaction proceeded according to eqn. (1). However, the product obtained by igniting the sample under an oxygen pressure of 101.3 kPa did not contain carbon and the final mass agrees with the calculated value based on eqn. (1). The excess mass gain is thus attributed to the precipitation of carbon as represented in

$$ZrC_XO_Y + [(4-Y)/2]O_2 \longrightarrow ZrO_2 + (X-1)C + CO_2 \qquad (7)$$

The masses read at each temperature for the calculation of the reacted fraction α were corrected for the excess carbon. The excess mass, however, was lost on subsequent heating. The initial excess mass gain could be due to the dissolution of oxygen in ZrC leading to the formation of oxycarbide. ZrC could accommodate oxygen up to 60% of the interstitial positions without changing its permanent structure [4].

The change in oxygen pressure from 5 to 50 kPa caused a significant rise in the rate of reaction as seen

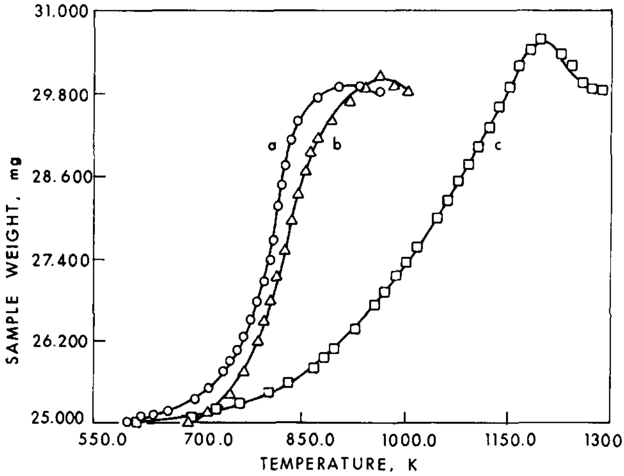

Fig. 1. Mass *vs.* temperature during the oxidation of ZrC under varying oxygen pressures: curve a, 50 kPa; curve b, 20 kPa; curve c, 5 kPa.

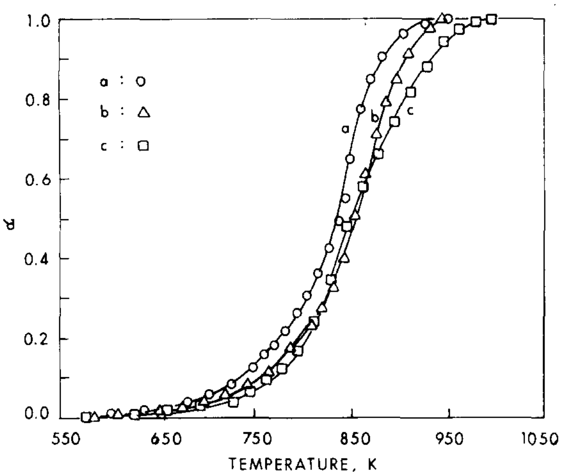

Fig. 2. Dependence of reacted fraction α on temperature with the variation in heating rate under 20 kPa oxygen pressure: curve a, ○, 5 K; curve b, △, 10 K; curve c, □, 15 K.

in Fig. 1. In all the cases the product oxide contained free carbon at the completion of the reaction but the amount decreased with the increase in the oxygen partial pressure. The temperature for the completion of the reaction also depended on the partial pressure. As seen in Fig. 1, the reaction under all the partial pressures initiated at the same temperature but terminated at different temperatures. The variation in heating rate did not influence the rate of the reaction and the inception temperature in each case was the same as seen in Fig. 2. The results of kinetic evaluation of the data are given in Tables 1 and 2. The data under 103 kPa oxygen pressure were not evaluated for kinetic parameters because the sample ignited.

The mass gain curves obtained in this work obey the following equation as proposed by Ginstling and Brounshtein [13]:

$$g(\alpha) = 1 - (2/3)\alpha - (1-\alpha)^{2/3} \tag{8}$$

This equation corresponds to a diffusion-controlled mechanism taking into account the volumes of both the reactant and the product independently.

The activation energies of the reaction under isothermal and non-isothermal heating conditions were evaluated as 131.8 kJ mol^{-1} and 116.7 kJ mol^{-1} respectively. These values are in reasonable agreement with 125 kJ mol^{-1} for the parabolic oxidation of Zr metal where oxygen diffuses through the oxide layer [14]. This suggests that oxygen diffusion into the matrix is predominantly rate determining in the present study. A higher activation energy of 292 kJ mol^{-1} was reported by Barnier and Thevenot [2] for an oxygen pressure of 13 kPa in the temperature range 673–1273 K for a diffusion-controlled mechanism. They observed the mechanism to change to phase boundary controlled during the later part of the reaction with an activation energy of 186 kJ mol^{-1}. They found that the reaction was pressure dependent. Bartlett *et al.* [5] studied the oxidation reaction under 1 atm oxygen pressure on the assumption that the reactant particles are spherical and proposed two different mechanisms to explain the complete reaction. The initial stages of the reaction were controlled by the phase boundary rate equation with an activation energy of 192.5 kJ mol^{-1} followed by a diffusion-controlled rate equation with an activation energy of 221.7 kJ mol^{-1}. However, these values are higher than the data of Shimada and Ishii [4] as well as the values obtained in the present study. Shimada and Ishii [4] observed two different rates for the reaction at different temperatures. They observed the precipitation of carbon at the end of the reaction and proposed a diffusion-controlled mechanism followed by surface reaction as the two rate-controlling processes at different stages of reaction. They evaluated two activation energies: 138 kJ mol^{-1} for the reaction below 743 K and 180 kJ mol^{-1} above 743 K. This change in the rate was attributed to the temperature of crystallization of cubic ZrO_2 at 743 K. For the diffusion model they [2, 4, 5] used Jander's rate equation for fitting of kinetic data apparently with the assumption that the volume ratio of the product and the reactant is unity. This equation was derived from the parabolic rate equation $kt = \alpha^2$, which was applicable for the reactions occurring on planar surfaces whose area remains constant throughout the progress of the reaction.

TABLE 1. Kinetic data on the oxidation of ZrC under non-isothermal heating conditions (α = 0.2–0.9)

Oxygen pressure (kPa)	Heating rate (K min^{-1})	$g(\alpha)$	E_a (kJ mol^{-1})	Z (s^{-1})
5.0	5	$1-(2/3)\alpha-(1-\alpha)^{2/3}$	142.3	5.6×10^{12}
20.0	5	$1-(2/3)\alpha-(1-\alpha)^{2/3}$	126.7	1.2×10^{10}
20.0	10	$1-(2/3)\alpha-(1-\alpha)^{2/3}$	114.9	1.8×10^{9}
20.0	15	$1-(2/3)\alpha-(1-\alpha)^{2/3}$	109.1	1.3×10^{9}
50.0	5	$1-(2/3)\alpha-(1-\alpha)^{2/3}$	99.8	2.7×10^{8}

TABLE 2. Oxidation of ZrC under isothermal conditions: rate constants, activation energy and pre-exponential factor for the Arrhenius expression $k = Z\exp(-E_a/RT)$

Temperature (K)	$k\times10^3$
758	8.06
773	12.03
788	17.77
803	25.99

Activation energy E_a = 131.8 kJ mol^{-1}; pre-exponential factor $Z = 8.5\times10^6$.

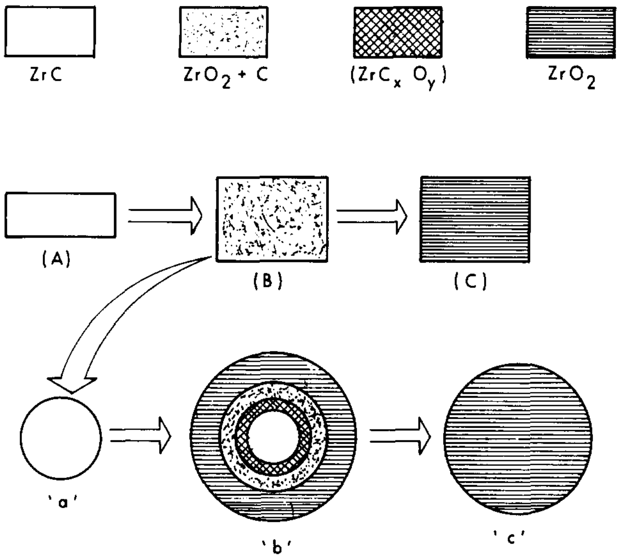

Fig. 3. Mechanistic model for the oxidation of ZrC to ZrO_2.

As the volume ratio of the product to reactant is more than unity in the present study Jander's eqn. (2) is not applicable for the treatment of data. Physical examination of the product did not reveal any unreacted substrate as a separate layer and hence bulk diffusion of the gas was assumed to be faster and the solid–gas reaction on each particle thus became important. If the reaction is considered to occur on each particle of spherical geometry with a monotonically decreasing surface area, as the reaction advances, any rate equation based on a parabolic rate law such as eqn. (2), as suggested by previous workers [4, 5], cannot be used to fit the data. This rate equation was discarded in the present study in favour of an equation relating the growth of a product layer having a different radius to that of the reactant. The progress of the reaction at various stages during bulk diffusion is shown in the form of a model (Fig. 3, stages A–C). The progress of the reaction occurring on each particle is also represented in Fig. 3 (stages a–c). The mechanistic models are based on the physical examination of the product, carbon content and X-ray diffraction (XRD) of the products during the course of reaction as well as the final products. The XRD patterns recorded at various reaction temperatures corresponding to different reacted fractions α are shown in Fig. 4. The growth in the intensity of the lines belonging to cubic ZrO_2 is clearly seen.

Although oxycarbide was reported to form as an intermediate species it could not be characterized in

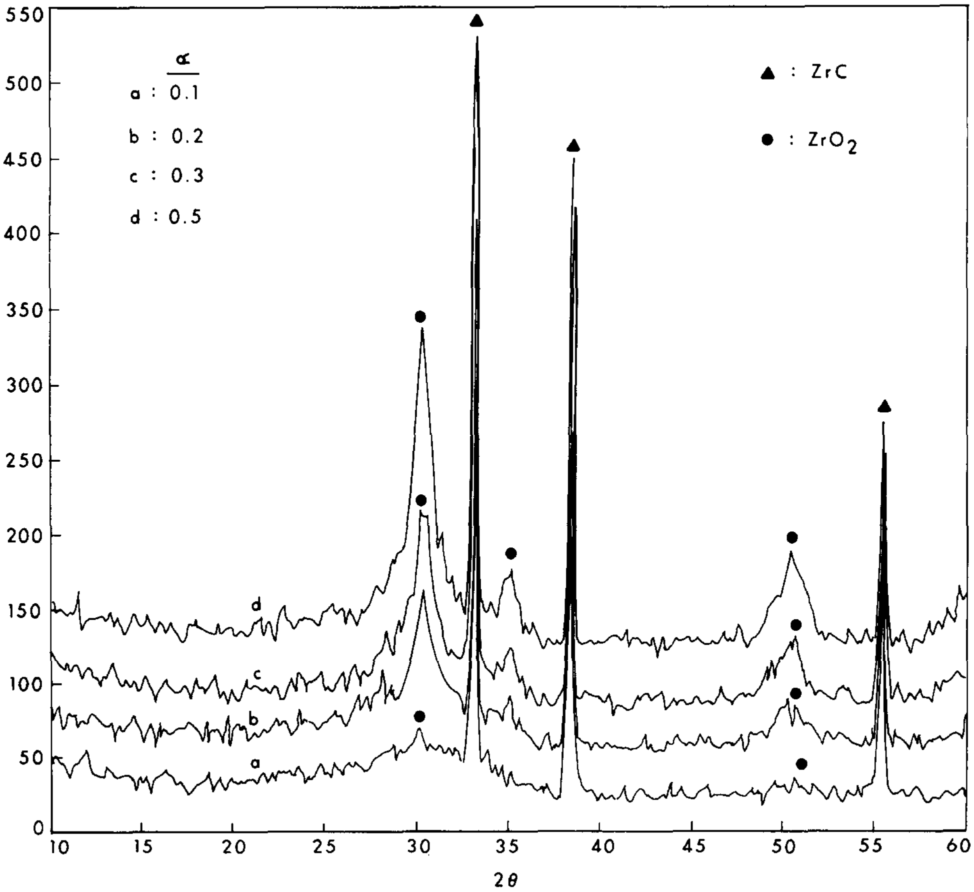

Fig. 4. XRD patterns of the products at various reacted fractions α.

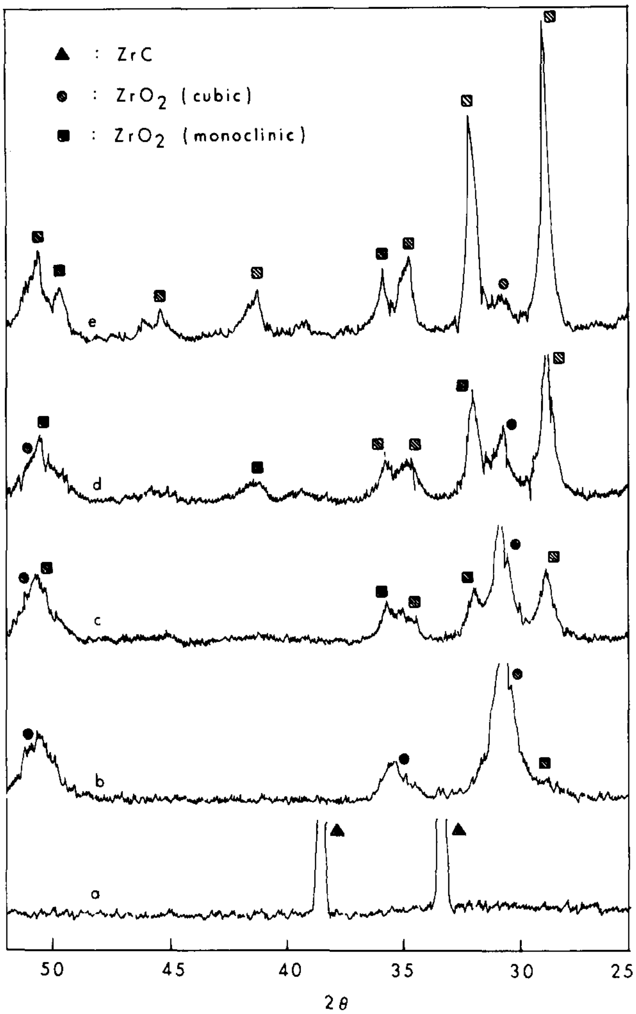

Fig. 5. XRD patterns of the products during the conversion of ZrC to ZrO_2 (monoclinic): spectrum a, ZrC (298 K); spectrum b, ZrO_2 (cubic, below 923 K); spectra c and d, ZrO_2 (cubic) + ZrO_2 (monoclinic) at above 923 K; spectrum e, ZrO_2 (monoclinic, above 1073 K).

the present study. The XRD patterns recorded on the samples collected at various fractions reacted did not exhibit any additional peak other than those belonging to ZrC or ZrO_2 as seen in Fig. 5. The conversion of ZrC to cubic ZrO_2 and then to monoclinic phase is seen in the XRD pattern recorded on samples heated at various temperatures. However, the precipitation of free carbon, a part of which was retained until the complete conversion of ZrC to ZrO_2 occurred, gives credence to the theory that the slow diffusion of oxygen into the matrix could lead to the formation of free carbon. The oxidation of carbon, being an altogether independent process, does not influence the diffusion of oxygen as the rate governing process.

As given in Section 2.1.1, transport of atomic oxygen into ZrC lattice appears to be a plausible explanation for the diffusion process but the rate of reaction is governed by eqn. (7). Since carbon was observed in ZrO_2 as a separate phase and its diffusion in the oxide matrix was negligible, the counterdiffusion of solid carbon or gaseous CO_2 cannot become the rate-dictating processes.

At the oxidation temperatures used in this study the stable phase of pure ZrO_2 is expected to have a monoclinic structure. However, the XRD patterns as given in Fig. 4 indicated that the product has a cubic zirconia phase which otherwise is stable above 2173 K [5]. ZrO_2 was reported to be monoclinic at room temperature with a transition to tetragonal at 1443 ± 20 K and from tetragonal to cubic at 2558 ± 15 K [15]. Blumenthal [16] has attributed the stabilization of the cubic structure to the presence of small amounts of residual carbon as impurity. It was observed in the present work that the stabilization of the cubic structure by carbon was limited to a temperature of 1023 K. The transformation of cubic to monoclinic phase as a consequence of the decrease in carbon content is indicated in the XRD study of the samples collected at various temperatures as shown in Fig. 5.

The presence of carbon was found to be essential for the stabilization of ZrO_2 cubic phase. This was confirmed from the experiments by heating the mixtures of ZrO_2(cubic) + C samples in oxygen-free atmosphere. The products were XRD analysed. Above 1073 K, the ZrO_2 monoclinic phase appeared together with the cubic phase in spite of the presence of carbon. Lattice parameters were calculated as 5.123 ± 0.006 Å for the cubic phase.

5. Conclusions

(1) the conversion of ZrC to ZrO_2 is controlled by diffusion of oxygen through the formation of oxycarbide as the intermediate.

(2) Free carbon was found to have been associated with ZrO_2 during the course of reaction which ultimately escaped as CO_2 when the reaction temperature exceeded 1073 K.

(3) The cubic ZrO_2 phase was observed below 1073 K and changed to monoclinic thereafter on further heating.

(4) A kinetic model based on a non-parabolic mechanism was used to fit the data and to evaluate the kinetic parameters.

(5) A mechanistic model was proposed to explain the progress of the reaction.

Acknowledgments

The authors are thankful to Dr. D.D. Sood, Director, Radiochemistry and Isotope Group, BARC, for helpful discussions. They are also thankful to Dr. H.C. Jain, Head, Fuel Chemistry Division, for constant encouragement.

References

1 Hj. Matzke, *Advanced LMFBR Fuels*, North-Holland, Amsterdam, 1986, Chap. 5, p. 286.

2 P. Barnier and F. Thevenot, *Eur. J. Solid State Inorg. Chem., 25* (5–6) (1988) 495.

3 Yu. D. Afomin, N. Shalaginov and A.R. Beketov, *Zh. Prikl. Khim., 56* (1983) 2185.

4 S. Shimada and T. Ishii, *J. Am. Ceram. Soc., 73* (10) (1990) 2804.

5 R.W. Bartlett, M.E. Wadsworth and I.B. Cutler, *Trans. Metall. Soc. AIME, 227* (1963) 467.

6 V.A. Zhilyaev and L.Kh. Askarova, *Izv. Akad. Nauk SSSR, Neorg. Mater., 23* (5) (1987) 788.

7 A.S. Shevchenko, R.A. Lyutikov, R.A. Andrievskij and V.A. Terekhova, *Poroshk. Metall.*, 1980, p. 64.

8 A.K. Kuriakose and J.L. Margrave, *J. Electrochem. Soc., 111* (7) (1964) 827.

9 J. Zsako, *J. Phys. Chem., 72* (1968) 2406.

10 P.V. Ravindran, *Thoermochim. Acta, 39* (1980) 135.

11 C.D. Doyle, *J. Appl. Polym. Sci., 5* (1961) 285.

12 F. Skvara and V. Satava, *J. Therm. Anal., 2* (1970) 325.

13 A.M. Ginstling and B.I. Brounshtein, *J. Appl. Chem. USSR (Engl. Transl.), 23* (1950) 1327.

14 W.W. Smeltzer, R.R. Haering and J.S. Kirkaldy, *Acta Metall., 9* (1961) 880.

15 K.A. Romberger, C.F. Baes, Jr. and H.H. Stone, *J. Inorg. Nucl. Chem., 29* (1967) 1619.

16 W.B. Blumenthal, *The Chemical Behavior of Zirconium*, Van Nostrand, New York, 1958, p. 46.